Interstellar Abundances in the Magellanic Clouds[1]

Daniel E. Welty (University of Chicago)
J. Chris Blades (Space Telescope Science Institute)
Priscilla C. Frisch (University of Chicago)
Lewis M. Hobbs (University of Chicago)
James T. Lauroesch (Northwestern University)
George Sonneborn (Goddard Space Flight Center)
Donald G. York (University of Chicago)

1. Introduction

Studies of the interstellar medium (ISM) in the Magellanic Clouds (MC) offer the prospect of interesting comparisons both with the ISM in our own Galaxy and with the absorption-line systems (ALS) seen in the spectra of distant QSO's. For these two nearby galaxies, we may obtain a global view of the interrelationships between the stellar component and the various phases of the ISM, though at somewhat lower spatial resolution than for our Galaxy. Elemental abundances have been determined for both gaseous nebulae and stars of different spectral types in the LMC and SMC, providing both clues to the nucleosynthetic history of the two galaxies and benchmarks for deducing depletions in the MC ISM. Relative to the Sun, the LMC and SMC have lower overall metallicities, by about 0.3 and 0.6 dex, respectively, with some differences in the relative abundances of the lightest and heaviest elements (e.g., Russell & Dopita 1992). The ISM in both MC appears to be characterized by generally lower dust-to-gas ratios than those commonly found locally in our Galaxy; after accounting for the lower metallicities, the dust-to-metals ratios also appear to be lower in the MC. In the SMC, and near 30 Dor in the LMC, the selective extinction due to the dust is typically significantly steeper in the far-UV than the "average" Galactic extinction, with a weaker 2200 Å bump; elsewhere in the LMC, however, the extinction is more similar to the Galactic average (e.g., Fitzpatrick 1989). Since the QSOALS also generally have sub-Solar metallicities and low dust-to-gas ratios (Pettini et al 1994; Lu et al. 1996), comparisons between the MC ISM and the QSOALS may also aid in disentangling the effects of nucleosynthetic history and dust depletion contributing to the gas-phase abundances observed in the QSOALS (Lauroesch et al. 1996: Welty et al. 1997).

In the Galactic ISM, different patterns of relative gas phase abundances seem to be associated with different physical environments, as characterized either by mean line of sight hydrogen density $< n_{\rm H} >$ or by the fraction of hydrogen in molecular form f(H_2) (e.g., Jenkins 1987; Cardelli 1994; Savage & Sembach 1996). If the Galactic ISM is well mixed, then the differences in gas phase abundance reflect primarily differences in depletion into dust grains. The most severe depletions are found in lines of sight with the largest mean densities and largest f(H_2); the least severe depletions are observed for halo clouds and for high-velocity clouds in which the grains apparently have been largely disrupted; intermediate depletions are found for the warm, diffuse disk clouds. These patterns [cold, dense cloud (C), warm, diffuse cloud (W), and halo cloud (H)] presumably represent a continuum of possible depletion patterns reflecting both the history of the clouds and local physical conditions, but they are useful for rough characterization of

[1]Poster presented at IAU Symposium 190 — New Views of the Magellanic Clouds (Victoria, BC; 1998 July)

the conditions in the gas. Furthermore, the overall level of depletion seems correlated with the pattern of depletion.

In this poster, we discuss the elemental abundances found for the predominantly neutral IS clouds — located in the Galactic disk and halo, in the SMC or LMC, and (perhaps) in between — along the lines of sight to Sk 108 in the SMC and to SN 1987A in the LMC. We will compare the abundances in the MC ISM with those found for IS clouds in various Galactic environments and with those found for QSOALS at redshifts $0.7 \lesssim z \lesssim 3.4$. Since the ratios of the column densities of singly-ionized species that are dominant in H I regions apparently yield reasonably accurate relative elemental abundances even when some ionized (H II) gas is present, we will use relative gas-phase abundances normalized to Solar ratios — e.g., [X/Zn] = log[N(X II)/N(Zn II)] – (A_X – A_{Zn}), where A_X is the log of the Solar abundance of element X — to characterize the various groups of IS components discerned in the observed spectra. In general, these abundance ratios reflect both the nucleosynthetic history of the gas and any selective depletion of elements into dust grains. Complete accounts of this work may be found in Welty et al. (1997) and Welty et al. (1998).

2. SMC (Sk 108)

Sk 108 is the second-brightest Wolf-Rayet binary in the SMC, and is located in the northeastern part of the main "bar" of the SMC, just south of the H II region N76A, apparently in the front part of the most distant of the four major SMC gas complexes identified in H I 21 cm emission surveys of the SMC (e.g., McGee & Newton 1981).

We obtained *HST* GHRS echelle-B and G160M spectra of Sk 108 on 1995 May 18-19. The individual FP-SPLIT subexposures were aligned and co-added; the resulting summed spectra were normalized via polynomial fits to the continuum regions. The echelle-B spectra have resolutions of 4.2±0.2 km s^{-1} (FWHM) and S/N ratios of 18-25 (Figure 1). The G160M spectra have a resolution of about 21 km s^{-1} and S/N ratios of 37-46.

The interstellar component structure (column densities, velocities, and line widths) was determined via a simultaneous, iterative, multi-component Voigt profile fit to the echelle profiles of Fe II λ2260, Fe II λ2586, Mn II λ2594, and Si II λ1808; 25 components were required to fit these four line profiles. The derived component velocities and line widths were used to fit the echelle profiles of the weaker Cr II and Zn II lines, and also to model the profiles of several other ions (O I, P II, S II, Ni II) seen in the lower resolution G160M spectra. The ratio N(Al III)/N(Al II) is about 0.1 for the Galactic components and about 0.2 for the SMC components (on average), suggesting that the gas is primarily neutral (H I), or at least that column density ratios for singly-ionized species should yield good estimates for the relative elemental abundances. The component velocities and various column density ratios suggest that we may identify five groups of components, each characterized by similar velocities and/or similar relative gas-phase abundances (Figure 2):

- The G1 components (-12 km s^{-1} $\lesssim v \lesssim$ 0 km s^{-1}) have relative abundances similar to those found for Galactic halo clouds; the velocities are also consistent with a halo location.
- The G2 components (7 km s^{-1} $\lesssim v \lesssim$ 50 km s^{-1}) are the dominant Galactic components, and likely arise in the Galactic disk. The relative abundances are similar to those found for warm, diffuse disk clouds, except that Si is slightly lower. While some C I is detected, the low N(C I)/N(Zn II) ratio

and the non-detection of C I in the excited fine-structure levels suggests that most of the gas is relatively warm and of low density.

- The S1 components (89 km s^{-1} $\lesssim v \lesssim$ 150 km s^{-1}) account for most of the total SMC column densities toward Sk 108, and may be associated with the H I complexes near 114 and 134 km s^{-1}. The relative abundances are similar to those found for Galactic halo clouds, except that Si is slightly higher and Ni slightly lower. Since C I is not detected, most of the gas is probably warm and of relatively low density.

- The S2 components (161 km s^{-1} $\lesssim v \lesssim$ 190 km s^{-1}) may arise in gas associated with the H I complex near 167 km s^{-1}. Strong 21 cm emisison at these velocities suggests that Sk 108 (with $v_{\rm rad} \sim$ 170 km s^{-1}) lies in front of most of the gas in this complex. The relative abundances may indicate slightly less severe depletions than those in the Galactic halo clouds and S1 components.

- The S3 components (203 km s^{-1} $\lesssim v \lesssim$ 210 km s^{-1}) may be associated with the 192 km s^{-1} H I complex. The relative abundances for Fe II, Si II, and S II are similar to those in the Galactic halo clouds. Comparison of those species with O I suggests that the gas may be roughly half ionized.

3. LMC (SN 1987A)

On 1987 February 23, Sk $-69°202$, a previously unremarkable B3 Ia star located about 20 arcmin SW of the core of the bright 30 Dor H II region in the LMC, was observed to explode as a supernova. Although the SN faded rapidly in the UV, it still was by far the brightest UV source in the LMC for a few days after its discovery, and it remained the brightest source at longer wavelengths for many months. Because it was situated fairly deep within the LMC, beyond much of the observed H I in its direction, it thus provided an unparallelled opportunity for investigating the intervening interstellar material — in the Galactic disk and halo, in the LMC, and in between.

High-resolution (FWHM $\sim$ 3-5 km s^{-1}) optical spectra of Na I, Ca II, and Ca I, obtained by Vidal-Madjar et al. (1987) and Magain (1987) using the ESO coudé auxiliary telescope and coudé echelle scanner, were used to model the lower resolution (FWHM $\sim$ 16-28 km s^{-1}) UV spectra of many other neutral and singly-ionized species obtained with the *IUE* satellite. A special flat-fielding procedure was used to enhance both the S/N ratios and the reliability of weak absorption features in the *IUE* spectra, enabling the detection of weak lines due (for example) to Mg I, P II, Cl I, and Ti II, as well as weak components for the stronger lines of other species. Profile fits to the high-resolution ESO spectra reveal (at least) 46 components, which may be associated with the ten component groups discernible in the UV spectra (Figure 3). Ultra-high resolution (FWHM $\sim$ 0.5 km s^{-1}) spectra of Na I and K I, obtained by Pettini & Gillingham (1988) using the AAT and a precursor to the UHRF, reveal additional components and provide strong constraints on the component temperatures.

From the UV spectra, we determined component group column densities for C I, Mg I, Mg II, Al II, Si II, P II, Cl I, Ti II, Cr II, Mn II, Fe II, Ni II, and Zn II — with 1σ uncertainties less than 0.1 dex in many cases. The component velocities, the patterns of relative elemental abundances [X/Zn] and [X/Fe], and various diagnostic ratios [e.g., N(Na I)/N(Zn II), N(Na I)/N(Mg I), N(Ca I)/N(Ca II)] can be used to estimate the locations and physical characteristics [N(H), T, n_e] of these component groups (Figure 4):

- Component group 2 (5 km s^{-1} $\lesssim v \lesssim$ 23 km s^{-1}) is due to gas in the Galactic disk. The relative abundances are very similar to those found for warm, diffuse disk clouds, and most of the diagnostic ratios also have values similar to those found for relatively warm, low density gas. The presence of several very narrow Na I components, the detection of CH, and the C I fine structure level populations indicate that there is some cold gas present as well, however.

- Component group 4 (56 km s^{-1} $\lesssim v \lesssim$ 90 km s^{-1}) is due to a mixture of warm and cool gas in the Galactic halo. The relative abundances suggest that group 4 may be a relatively rare example of essentially undepleted gas.

- Intermediate velocity groups 5 (110 km s^{-1} $\lesssim v \lesssim$ 140 km s^{-1}) and 6 (155 km s^{-1} $\lesssim v \lesssim$ 176 km s^{-1}) appear to have very similar properties, but are probably located in the Galactic halo and in the LMC, respectively, based on prior comparisons of H I 21 cm emission and optical absorption lines. For both groups, the relative abundances are very similar to those found for clouds in the Galactic halo. Enhanced Mg I and/or Ca I suggest that the clouds are warm, with $T \sim 4500$ K; the limit on n_e/n_H suggests that there is at least partial ionization of H.

- Component group 7 (191 km s^{-1} $\lesssim v \lesssim$ 225 km s^{-1}) is due to gas in the LMC, perhaps very close to the SN. The relative abundances are similar to those found for Galactic halo clouds. The various diagnostic ratios are typical of warm, low density disk clouds; T for the main subcomponent at 216 km s^{-1} is likely less than about 1500 K, however.

- Component groups 8 (238 km s^{-1} $\lesssim v \lesssim$ 255 km s^{-1}) and 9 (265 km s^{-1} $\lesssim v \lesssim$ 270 km s^{-1}), are probably located on opposite sides of the main LMC component group 10 (276 km s^{-1} $\lesssim v \lesssim$ 295 km s^{-1}), based on comparisons with observations of [N II] emission (Xu & Crotts 1995) and the structure inferred from light echoes (Xu et al. 1995). Group 10 is associated with the main H I disk ("D") component seen in 21 cm emission (Luks & Rohlfs 1992). The relative abundances, for all three groups, resemble most the pattern found for warm, low density disk clouds, consistent with the values of most of the diagnostic ratios. Enhanced Ca I in group 8 may indicate slightly warmer temperatures ($T \sim 5000$ K). Higher N(Na I)/N(Ca II) ratios, the presence of CH, and the C I fine structure level populations suggest that group 10 contains both cool and warm gas; line widths of Na I and K I may indicate that most of the gas has $T \lesssim 1500$ K.

4. MC Interstellar Abundances and Depletions

For the SMC (and the LMC), the relative abundances determined for emission nebulae and young stars are very similar to the relative abundances found for analogous Galactic objects, at least for the α-particle and Fe-peak elements (Russell & Dopita 1992). In particular, there is no significant enhancement of the α-particle elements, relative to the Fe-peak elements, nor is there any significant deficit of Mn, relative to the other Fe-peak elements. The average SMC (Sk 108) and LMC (SN 1987A) interstellar gas phase abundance ratios, relative to Zn, are summarized in Figure 5 (top). The SMC interstellar abundance pattern seen toward Sk 108 is very similar to that found for Galactic halo clouds, except that Si appears to be higher by about a factor of 2 and Ni lower by about a factor of 2.5. The abundance ratios for the main LMC interstellar component blend (group 10) seen toward SN 1987A are very similar to the ratios found for warm clouds in the Galactic disk, while the relative abundances in the "intermediate velocity" clouds along that line of sight resemble more those in the Galactic halo clouds. Since the ratios of the underlying total abundances for these elements in the SMC and LMC are similar to those found locally in our Galaxy, it is reasonable to conclude that the similar gas phase abundance patterns found in these three local galaxies are a reflection of similar depletion patterns, despite differences in overall metallicity, dust-to-gas ratio, and interstellar extinction curves. Furthermore, the $N_{\rm H}$ inferred for the LMC and SMC components, using the observed depletion patterns and the overall sub-solar metallicities of the two galaxies, are in good agreement with those based on measurements of Lyman α absorption (Fitzpatrick 1985; Fitzpatrick & Walborn 1990). This similarity in observed depletion patterns is particularly significant, in light of our relatively poor understanding of how grains form and how they evolve in the ISM (e.g., Draine 1990), and of previous speculations that dust could in principle have a different composition at lower metallicities and/or higher redshifts. While we have not found evidence for gas with "cold, dense cloud" depletions along these two MC lines of sight, the overall column densities and E(B-V) are relatively small in both cases. Detailed studies of additional LMC and SMC lines of sight, sampling different environments and larger total column densities, are needed in order to gauge the uniformity of the relative abundances within each galaxy and to search for gas with more severe depletions.

5. QSO Absorption-Line Systems

These results concerning the interstellar abundances in the SMC and LMC are also of some relevance for understanding the relative gas phase abundances observed in the QSOALS, which at redshifts 0.5 $\lesssim$ z $\lesssim$ 4.5 sample an appreciable fraction of the age of the Universe. A number of recent papers (e.g., Lauroesch et al. 1996; Lu et al. 1996; Pettini et al. 1997; Kulkarni, Fall, & Truran 1997; Vladilo 1998) have discussed the expectation that the total (gas plus dust) abundances in low-metallicity QSOALS might exhibit a pattern similar to that found for metal-poor Galactic stars. For Galactic metal-poor stars with [Fe/H] $\lesssim -1.0$, the α-particle elements (Ne, Mg, Si, S, Ar, Ca, and perhaps Ti) are enriched, relative to the even-Z Fe-peak elements (Cr, Fe, Ni, Zn), by roughly a factor 2-3. At least some odd-Z elements (e.g., Al, Mn) can be somewhat deficient, compared to the even-Z elements in the same nucleosynthetic group. These differences from Solar ratios are presumed due to differences in the time scales characterizing the sources of the various elements (primarily Type I vs. Type II supernovae). In general, it is necessary to consider the abundances of a number of elements, characterized by different nucleosynthetic history and depletion properties, in order to separate the two effects.

For the $\sim$35 damped Lyman α systems examined so far (mostly at z $\sim$ 1.5-2.5), the observed [Zn/H] seems to imply typical metallicites of $\sim 0.1 \times$ Solar, although there appears to be a wide range in [Zn/H] at any z (e.g., Pettini et al. 1994, 1997). The typically sub-Solar ratios of the abundances of such elements as Fe, Cr, and Ni, with respect to Zn, have generally been interpreted to indicate the presence of some depletion and dust in the QSOALS (e.g., Meyer et al. 1989; Pettini et al. 1994). Lu et al. (1996), however, recently suggested that the observed gas phase abundance ratios are more consistent with the pattern "expected" from nucleosynthetic processes alone, as exhibited by the Galactic metal-poor halo stars — and that there is no strong evidence for depletion. Pettini et al. (1997) countered that at the modest depletions implied by the observed [Cr/Zn] (only a factor $\sim$2, with a range at any z), the differences in depletion normally seen among various elements in the Galactic ISM (and the apparent correlation of depletion with condensation temperature) would be greatly reduced. The relative abundances would be rather similar to those found for the Galactic halo clouds; the halo cloud depletion pattern is thus likely to provide a more appropriate local comparison for the QSOALS. Pettini et al. also emphasized the significance of recognizing even such relatively small amounts of dust for a proper understanding both of the relationship between the high-z QSOALS and objects (galaxies) currently known at low z, and of the radiative transfer properties of the QSOALS. Since even such small amounts of dust can affect the observed relative gas phase abundances to a degree comparable to the effects expected from nucleosynthetic processes (i.e., factors of 2-3), the elemental enrichment history traced by the QSOALS cannot be reliably determined apart from an accurate assessment of the effects of depletion (Lauroesch et al. 1996).

In Figure 5, we compare relative heavy element abundances found in the interstellar media of the Galaxy, SMC, and LMC with those found for QSOALS. In the lower panel of the figure, we also show the relative abundances found in metal-poor Galactic halo stars at [Fe/H] ~ -1 (shown by asterisks). While all the systems are not represented in all the ratios and some ratios are known for only a small number of systems, these QSOALS abundance ratios (typically averages over multiple components) can be used for initial comparisons. The relative gas phase abundances of Si, Cr, Mn, Fe, and Ni in the QSOALS, with respect to Zn, are generally sub-Solar, and are very consistent with the pattern seen in Galactic halo clouds (and in the SMC interstellar gas), though a considerable range is exhibited for each; Ti may be slightly more abundant than in the halo clouds. The average QSOALS abundance ratios do not, in general, agree with those found for the metal-poor halo stars. If the underlying total abundances in the QSOALS have Solar ratios (as seems to be true for Cr, Fe, Ni, and Zn in the metal-poor halo stars), then the sub-Solar gas phase abundance ratios [X/Zn] found for the QSOALS would indicate the presence of some degree of depletion (as has often been inferred).

Additional insight may be gained by examining the abundance ratios observed for individual QSOALS (Figure 6). Some systems (e.g., 1946+7658, z = 1.74; 0528-2505, z = 2.14) appear to show relative abundances consistent with those in the metal-poor stars at [Fe/H] ~ -1, with little or no depletion ([Si/Zn] > 0, [Mn/Zn] $<$ [Fe/Zn], [Fe/Zn] ~ 0). For other systems (e.g., 0201+3634, z = 2.46; 0528-2505, z = 2.81), the pattern is very similar to that found for the Galactic halo clouds and for the SMC interstellar gas toward Sk 108 ([Mg/Zn] and [Si/Zn] $\lesssim 0$, [Cr/Zn] and [Fe/Zn] $\lesssim -0.5$). The two systems for which H_2 has been detected [0013-004, z = 1.97 (Ge & Bechtold 1997); 0528-2505, z = 2.81 (Foltz, Chaffee, & Black 1988)] both have relative heavy element abundances consistent with some depletion — as would be expected if the H_2 is formed on grain surfaces. While additional data for Mg, Al, Si, Ti, and Mn would clearly be valuable, it seems apparent that the QSOALS exhibit a range of relative abundance patterns, due to varying contributions from both different nucleosynthetic processes and depletion, just as they exhibit a range in metallicity. There does not seem to be any obvious correlation of abundance pattern with either redshift or metallicity.

Acknowledgements

We are grateful to A. Vidal-Madjar, P. Magain, and R. Stathakis for providing the high-resolution optical spectra of SN 1987A, and to the staff at STScI for their assistance with the observations of Sk 108. The UV spectra of SN 1987A were obtained under the *IUE* target of opportunity program for supernovae (R. Kirshner and N. Panagia, PI's). This work has been supported by NASA, largely through grant GO-5394.01-94A administered by STScI and through Long-Term Space Astrophysics grant NAG5-3228.

REFERENCES

Cardelli, J. A. 1994, Science, 265, 209

Draine, B. T. 1990, in The Evolution of the Interstellar Medium, ed. L. Blitz (San Francisco: PASP), 193

Fitzpatrick, E. L. 1985, ApJS, 59, 77

Fitzpatrick, E. L. & Walborn, N. R. 1990, AJ, 99, 1483

Foltz, C. B., Chaffee, F. C., & Black, J. H. 1998, ApJ, 324, 267

Ge, J. & Bechtold, J. 1997, ApJ, 477, L73

Jenkins, E. B. 1987, in Interstellar Processes, ed. D. J. Hollenbach & H. A. Thronson (Dordrecht: Reidel), 533

Kulkarni, V. P., Fall, S. M., & Truran, J. W. 1997, ApJ, 484, L7

Lauroesch, J. T., Truran, J. W., Welty, D. E., & York, D. G. 1996, PASP, 108, 641

Lu, L., Sargent, W. L. W., Barlow, T. A., Churchill, C. W., & Vogt, S. S. 1996, ApJS, 107, 475

Luks, Th. & Rohlfs, K. 1992, A&A, 263, 41

Magain, P. 1987, Nature, 329, 606

McGee, R. X. & Newton, L. M. 1981, Proc. Astron. Soc. Australia, 4, 308

Meyer, D. M., Welty, D. E., & York, D. G. 1989, ApJ, 343, L37

Pettini, M. & Gillingham, P. 1988, AAO Newsletter, No. 43

Pettini, M., King, D. L., Smith, L. J., & Hunstead, R. W. 1997, ApJ, 478, 536

Pettini, M., Smith, L. J., Hunstead, R. W., & King, D. L. 1994, ApJ, 426, 79

Russell, S. C., & Dopita, M. A. 1992, ApJ, 384, 508

Savage, B. D. & Sembach, K. R. 1996, ARA&A, 34, 279

Vidal-Madjar, A., Andreani, P., Cristiani, S., Ferlet, R., Lanz, T., & Vladilo, G. 1987, A&A, 177, L17

Vladilo, G. 1998, ApJ, 493, 583

Welty, D. E., Lauroesch, J. T., Blades, J. C., Hobbs, L. M., & York, D. G. 1997, ApJ, 489, 672

Welty, D. E., Frisch, P. C., Sonneborn, G., & York, D. G. 1998, ApJ, submitted

Xu, J. & Crotts, A. P. S. 1995, BAAS, 187, #45.08

Xu, J., Crotts, A. P. S., & Kunkel, W. E. 1995, ApJ, 451, 806

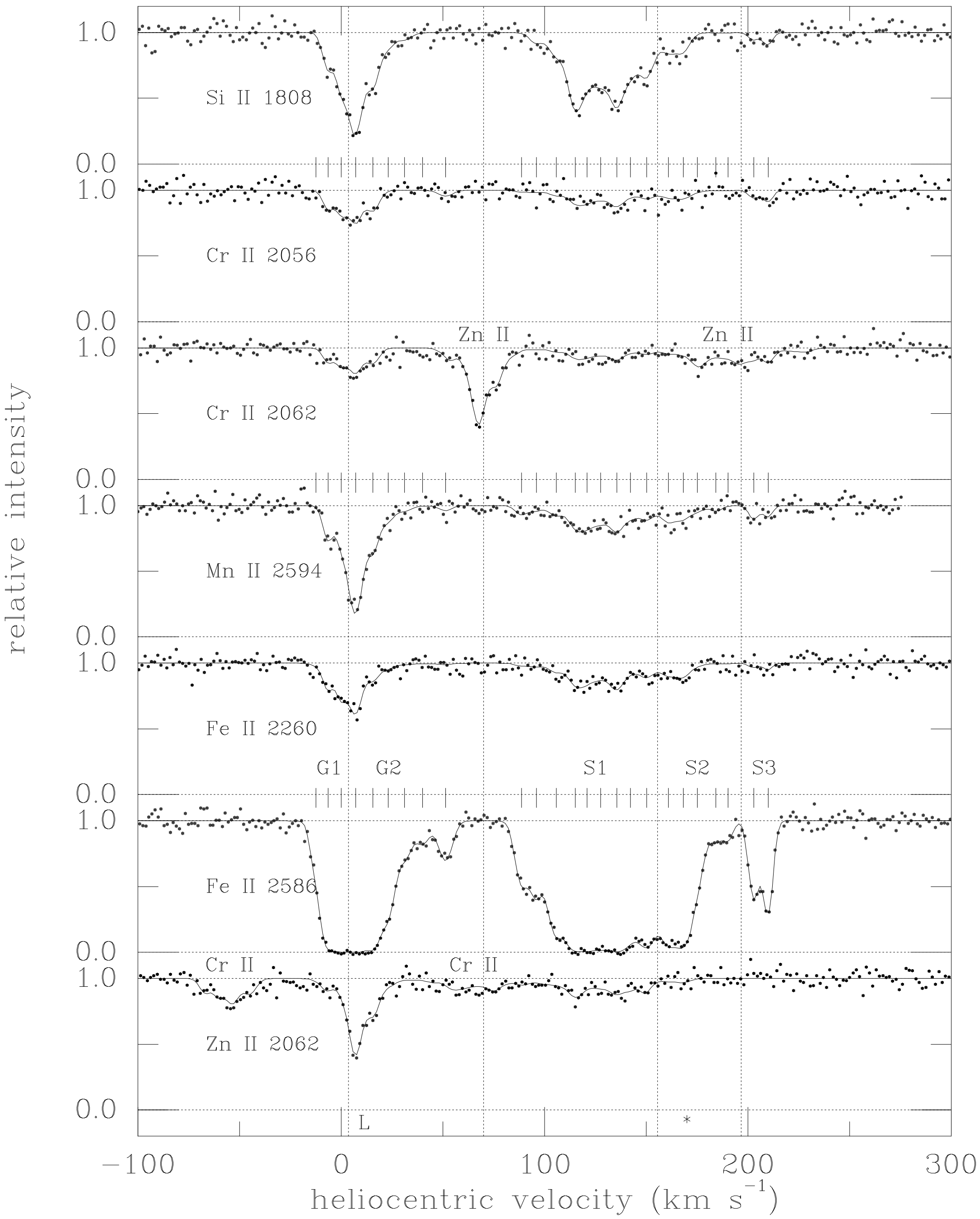

Fig. 1.— Interstellar absorption features along the line-of-sight to Sk 108 seen in GHRS echelle-B data (FWHM $\sim$ 4.2 km s^{-1}), plotted as relative intensity versus heliocentric velocity. Vertical dotted lines separate the five component groups (G1, G2, S1, S2, S3) identified via similar relative abundances and/or velocities in fits to the profiles. The smooth lines are the fits to the data (denoted by points); the individual components are noted by tick marks above Cr II λ2056, Mn II λ2594, and Fe II λ2586. Components at v $<$ 70 km s^{-1} arise in the Galactic halo and disk; components at v $>$ 70 km s^{-1} are due to gas in the SMC. Note that the Cr II and Zn II λ2062 components are interleaved, with Cr II at $-$62.5 km s^{-1} with respect to Zn II. The "L" at 11 km s^{-1} denotes $v_{\rm LSR}$ = 0 km s^{-1}; the asterisk at 170 km s^{-1} denotes the stellar velocity.

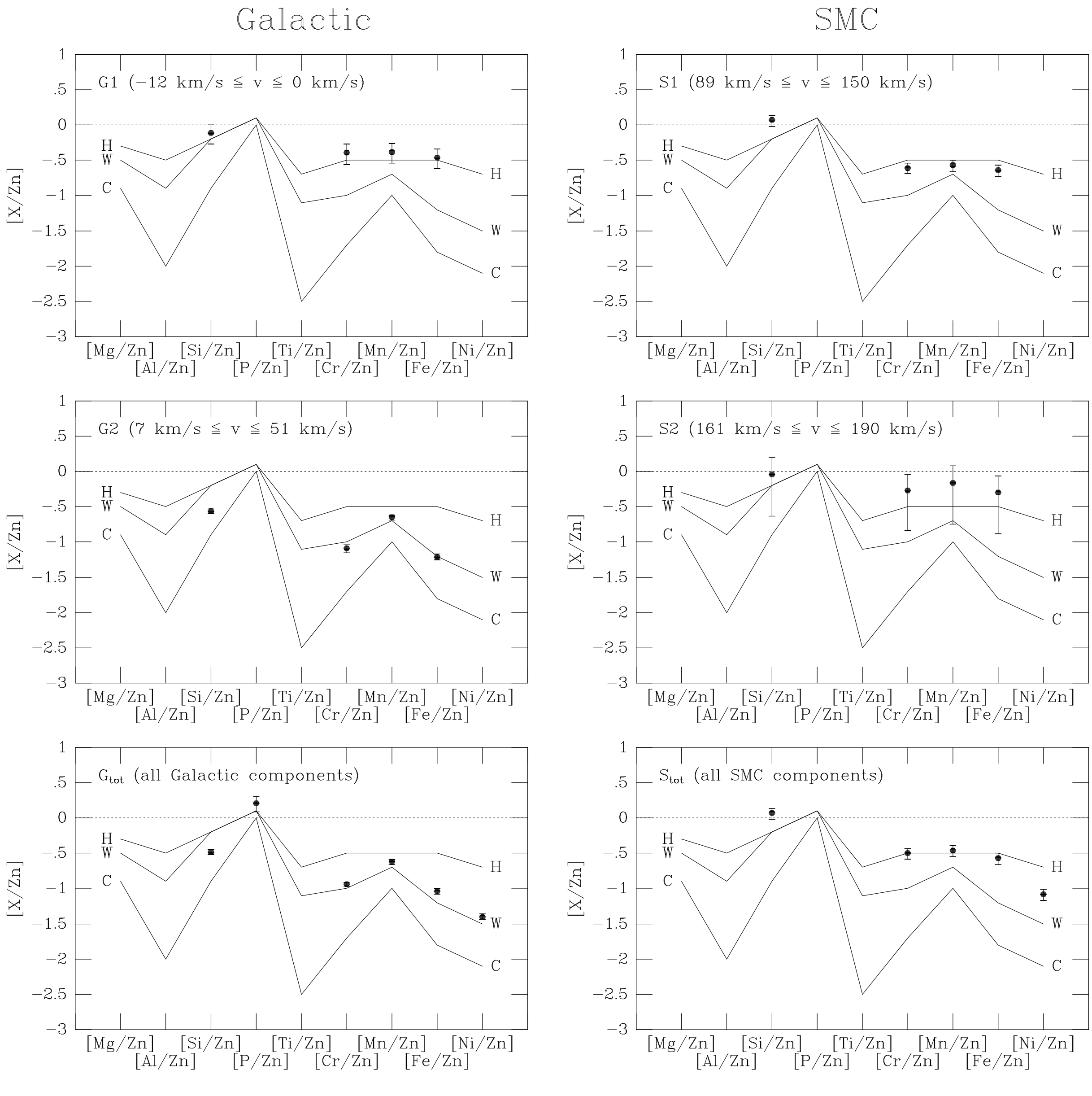

Fig. 2.— Relative gas phase abundances for Galactic (left) and SMC (right) component groups toward Sk 108, with respect to Zn, relative to Solar ratios [i.e., [X/Zn] = $\log[N(\mathrm{X\ II})/N(\mathrm{Zn\ II})] - (A_X - A_{Zn})$], compared to relative abundances found in Galactic cold (C), warm (W), and halo (H) clouds. Error bars are 1σ. Group G1 components probably arise in the Galactic halo; group G2 components probably arise in the Galactic disk, and contain most of the Galactic gas along the line of sight. The group S1 pattern resembles that of the Galactic halo clouds; the group S2 pattern suggests even less depletion. Most of the SMC gas along the line of sight is in the S1 components. Ni is somewhat underabundant, and Si somewhat overabundant, compared to the halo cloud pattern.

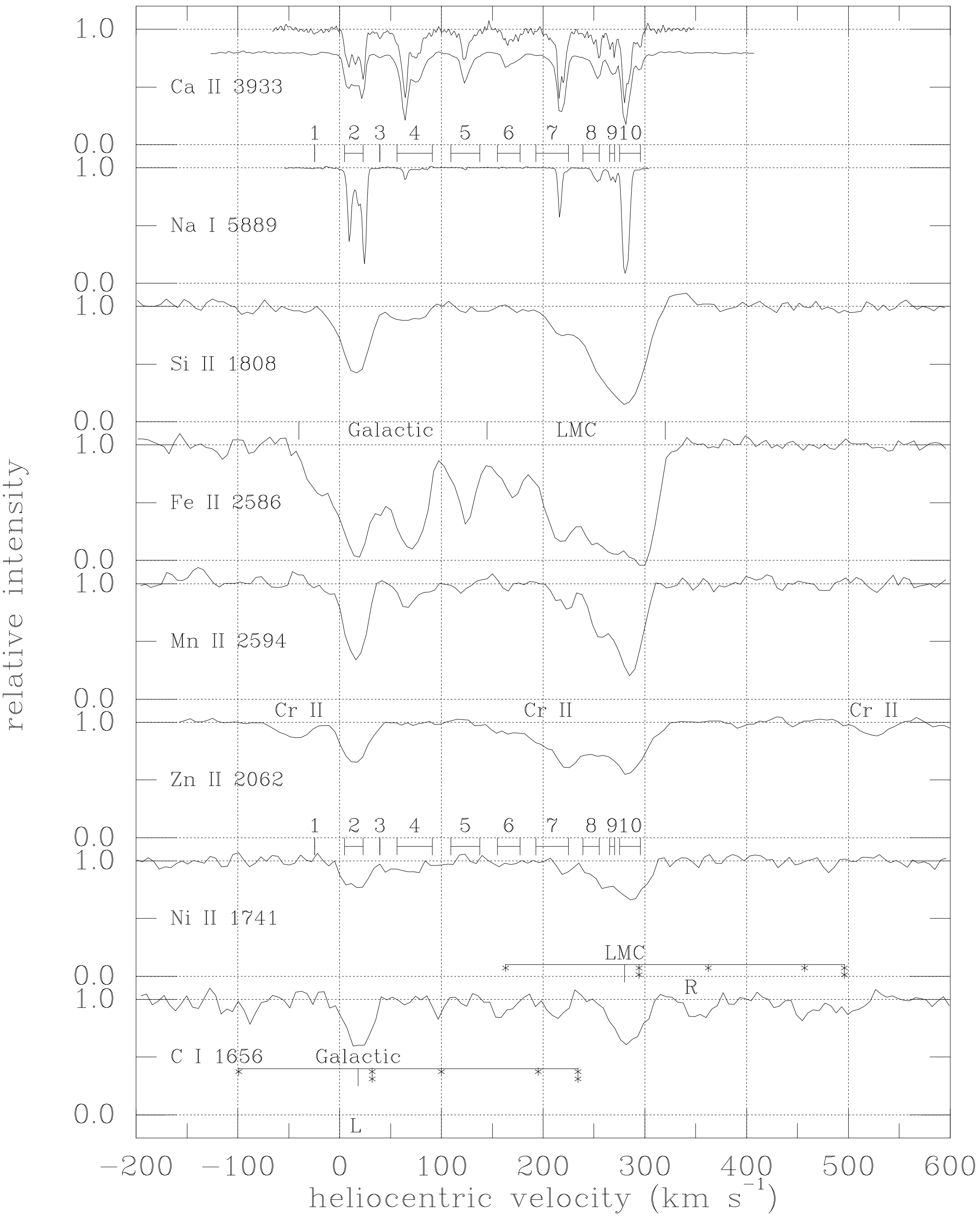

Fig. 3.— Spectra of selected optical and UV absorption lines seen toward SN 1987A. Upper Ca II spectrum and Na I D_2 spectrum are from Vidal-Madjar et al. (1987); lower Ca II spectrum is from Magain (1987). Component groups identified in fitting the optical lines are identified above the Na I and Ni II spectra; corresponding blends can be seen in the lower resolution UV spectra. Component groups 1-4 arise in the Galactic disk and halo; component groups 7-10 probably arise in the LMC. At the bottom, the velocities corresponding to the relative wavelengths of the C I excited states (* and **) associated with the main Galactic (2) and LMC (10) component blends are indicated. R denotes contamination from detector reseaux.

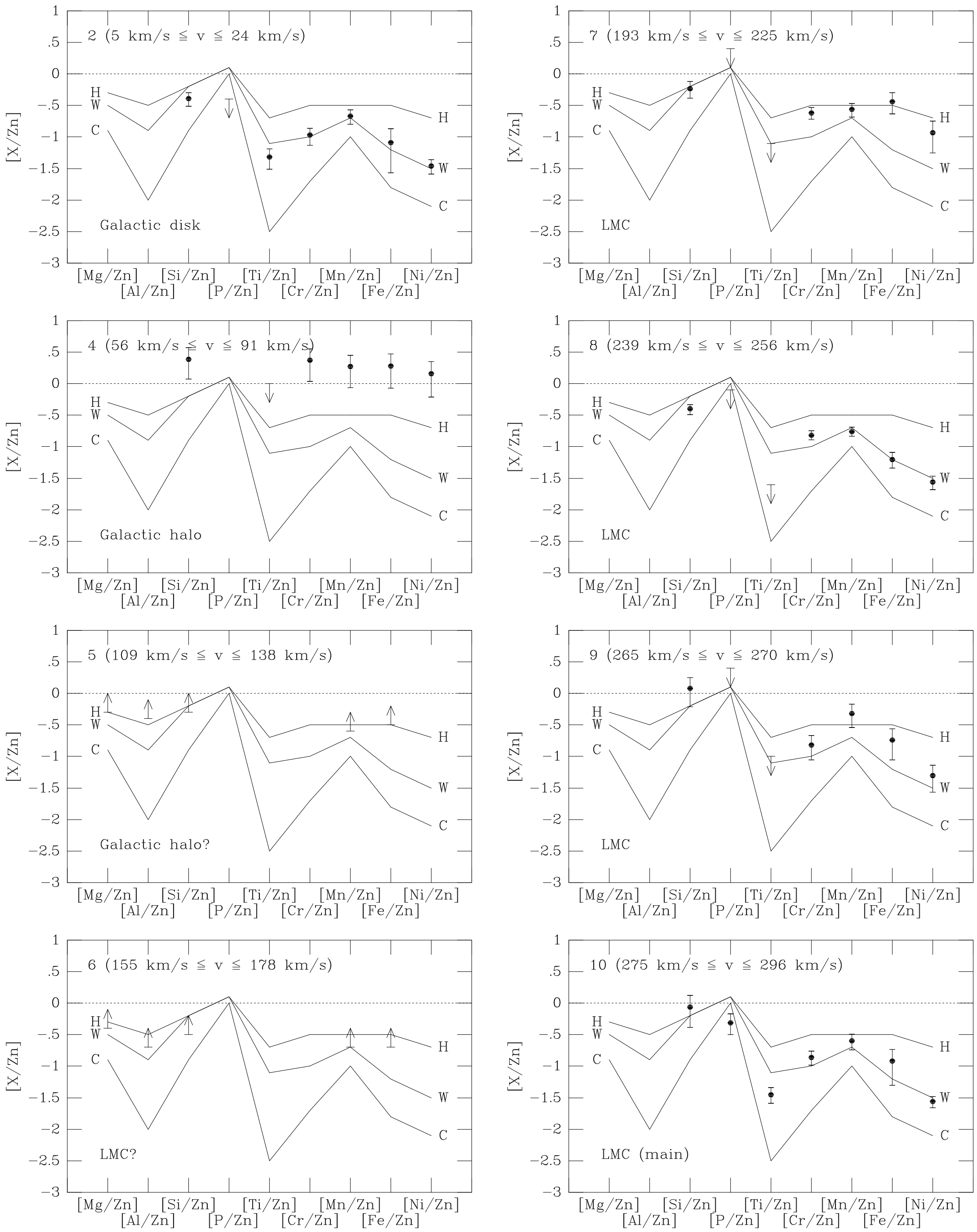

Fig. 4.— Relative gas phase abundances for various component groups (with respect to Zn, relative to Solar ratios), compared to relative abundances found in Galactic cold (C), warm (W), and halo (H) clouds. Error bars are 1σ; limits are 2σ. Component groups 2, 4, and (perhaps) 5 are due to gas in the Galactic disk and halo; component groups 6 through 10 are likely due to gas associated with the LMC.

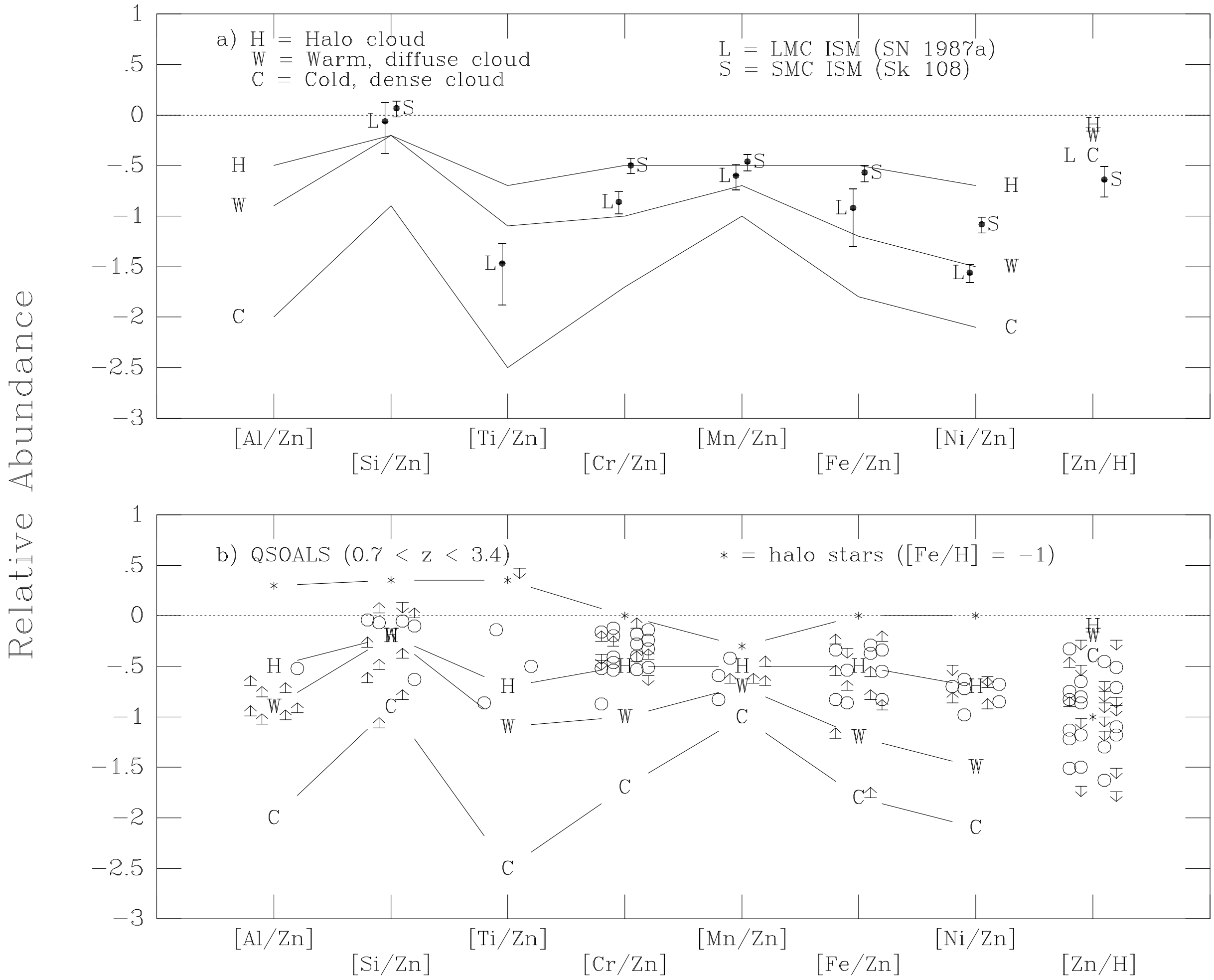

Fig. 5.— (a; top) Relative gas phase abundances for main LMC (SN 1987A) and SMC (Sk 108) component groups (with respect to Zn, relative to Solar ratios), compared to relative abundances found in Galactic cold (C), warm (W), and halo (H) clouds. These abundance patterns reflect both the nucleosynthetic history of the gas and any selective depletion. The [Zn/H] ratio is shown at the far right; the points for the LMC and SMC reflect primarily the lower than Solar metallicity of those systems. The pattern seen for the main LMC (L) component (blend) is similar to the Galactic warm cloud pattern; the SMC (S) components resemble more the halo cloud pattern. Since the stellar abundance ratios are not much different from Solar for these elements in the LMC and SMC, the interstellar depletion patterns may also be similar. (b; bottom) Relative gas phase abundances for a small number of QSOALS ($0.7 \lesssim z \lesssim 3.4$; data from current literature; see Welty et al. 1997 for references). A range in [Zn/H] is apparent, though all [Zn/H] are really upper limits, since ionized H could be present. The overall pattern of relative abundances, with respect to Zn, is similar to the halo cloud and SMC ISM patterns, but not to the halo star pattern at [Fe/H] ~ -1 (asterisks); slight differences suggest both nucleosynthetic history and depletion effects may contribute to the observed abundances. Note that all systems are not represented in all ratios; typical 1σ uncertainties are ±0.15; limits are 4σ.

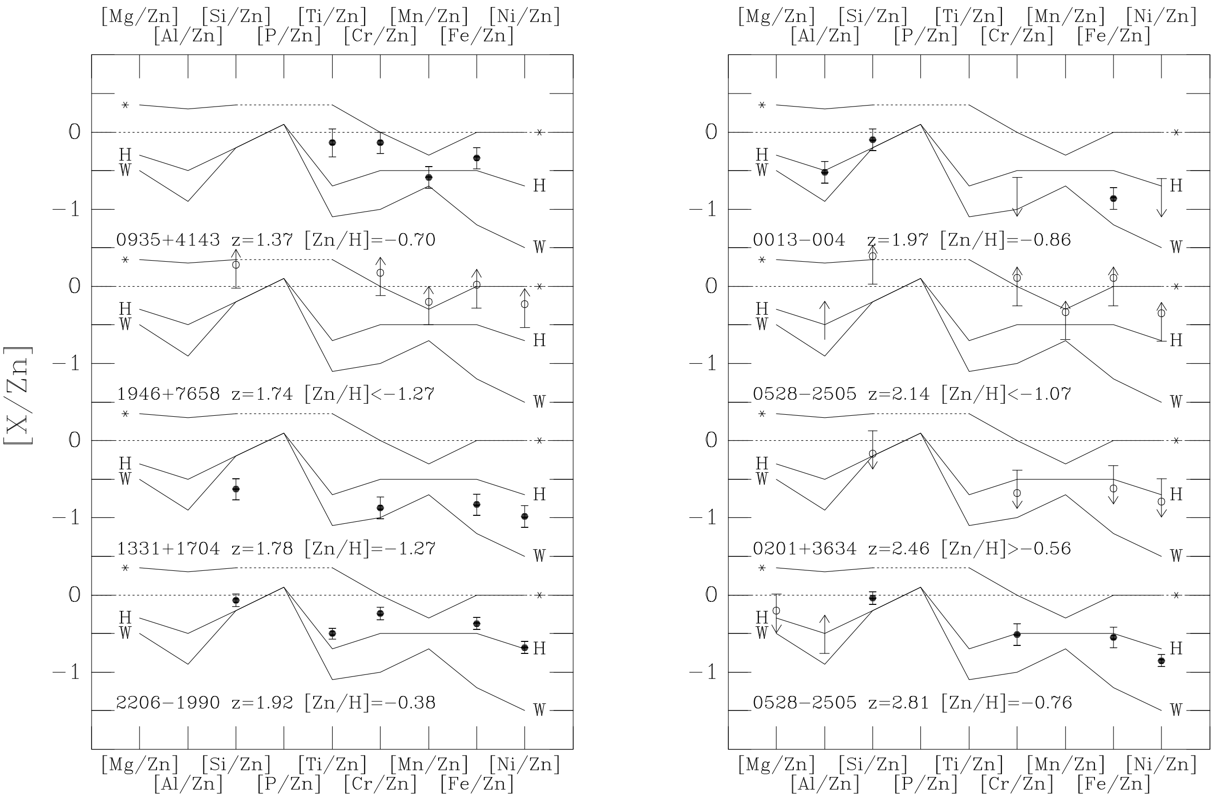

Fig. 6.— Relative gas phase abundances for some individual QSOALS, with respect to Zn, relative to Solar photospheric values [i.e., $[\mathrm{X/Zn}] = \log[N(\mathrm{X\,II})/N(\mathrm{Zn\,II})] - (A_X - A_{Zn})$], compared to relative abundances found for Galactic warm (W) and halo (H) clouds and for Galactic metal-poor stars (*) with [Fe/H] ~ -1. Limits with a cross-bar denote cases where a limit (4σ) is available for one of the two species (generally Zn), while limit with no cross-bar (one [Al/Zn] point) is based on limits for both species. Possible 2-4σ detections or estimated "likely" values are indicated by circles superposed on the arrows denoting the 4σ limits. Error bars are 1σ; representative column density errors of ± 0.1 dex have been assumed for several systems. A range of relative abundance patterns, presumably reflecting different nucleosynthetic history and depletion effects, is apparent. Some (1946+7658, z=1.74; 0528-2505, z=2.14) may have metal-poor star base abundances and negligible depletion, while others (0201+3634, z=2.46; 0528-2505, z=2.81) may have solar base abundances and halo cloud depletions. References for these data are given in Welty et al. 1997.

Table 1. Component Groups toward Sk 108 (SMC)

Group	Velocity Range (km s^{-1})	Location	log[N(H)][a] (cm^{-2})	Depletion Pattern[b]	Comments
G1	-12 to 0	Galactic halo	19.4	H	
G2	7 to 51	Galactic disk	20.5	W	warm, low density (no C I*, low C I/Zn II)
S1	89 to 150	SMC	20.6	H	warm, low density (no C I) H I complexes at 114, 134 km s^{-1}
S2	161 to 190	SMC	19.6	H	H I complex at 167 km s^{-1} (Sk 108 mostly foreground)
S3	203 to 210	SMC	19.2	H?	H I complex at 192 km s-1 half ionized?

[a]Inferred from abundance patterns and overall metallicities for Galaxy or SMC — values are consistent with total N(H) derived from Lyman α absorption.

[b]H = Galactic halo cloud pattern; W = Galactic warm, diffuse cloud pattern.

Table 2. Component Groups toward SN 1987A (LMC)

Group	Velocity Range (km s^{-1})	Location	log[N(H)][a] (cm^{-2})	Depletion Pattern[b]	Comments
2	5 to 23	Galactic disk	20.7	W	mixed cool and warm (C I fine structure, line profiles)
4	56 to 90	Galactic halo	19.0	N	mixed cool and warm (line profiles) no depletion
5	110 to 140	Galactic halo?	18.9	H	$T \sim 4500$ K (enhanced Ca I, Mg I) partially ionized ($\log[n_e/n_H] > -2.4$ dex)
6	155 to 176	LMC?	19.1	H	$T \sim 4500$ K (enhanced Ca I, Mg I)
7	191 to 225	LMC	20.1	H	mixed cool and warm (line profiles) $<$ 100 pc from SN?
8	238 to 255	LMC	20.7	W	mixed cool and warm (line profiles) 90-140 pc from SN
9	265 to 270	LMC	20.3	W	mixed cool and warm (line profiles) 535-585 pc from SN
10	276 to 295	LMC	21.25	W	mostly cool? (line profiles, CH, C I, Na I/Ca II) 340-380 pc from SN; main LMC comp

[a]Inferred from abundance patterns and overall metallicities for Galaxy or LMC — values are consistent with total N(H) derived from Lyman α absorption.

[b]H = Galactic halo cloud pattern; W = Galactic warm, diffuse cloud pattern; N = no depletion.